On the reflectance spectroscopy of snow

Alexander Kokhanovsky(1), Maxim Lamare(2,3), Biagio Di Mauro(4), Ghislain Picard (2), Laurent Arnaud (2), Marie Dumont (3), François Tuzet (3,2), Carsten Brockmann(5), Jason E. Box(6)

(1) VITROCISET, Bratustrasse 7, D-64293 Darmstadt, Germany

(2) UGA, CNRS, Institut des Géosciences de l'Environnement (IGE), UMR 5001, Grenoble, 38041, France

(3) Meteo-France–CNRS, CNRM UMR 3589, Centre d'Etudes de la Neige, Grenoble, France

(4) Department of Earth and Environmental Sciences, University of Milano-Bicocca, Piazza della Scienza, 1 20126 Milan, Italy

(5) Brockmann Consult, Max Planck Strasse 2, Geesthacht, Germany

(6) Geological Survey of Denmark and Greenland (GEUS), Copenhagen, Denmark

Abstract
We propose a system of analytical equations to retrieve snow grain size and absorption coefficient of pollutants from snow reflectance or snow albedo measurements in the visible and near-infrared regions of the electromagnetic spectrum, where snow single scattering albedo is close to 1.0. It is assumed that ice grains and impurities (e.g., dust, black and brown carbon) are externally mixed, the snow layer is semi-infinite and vertically and horizontally homogeneous. The influence of close–packing effects on reflected light intensity are assumed to be small and ignored. The system of nonlinear equations is solved analytically in the assumption that impurities have the spectral absorption coefficient , which obey the Angström power law, and the impurities influence the registered spectra only in the visible and not at near-infrared (and vice versa for ice grains). The theory is validated using spectral reflectance measurements and albedo of clean and polluted snow at various locations (Antarctica Dome C, European Alps). The technique to derive the snow albedo (plane and spherical) from

reflectance measurements at a fixed observation geometry is proposed. The technique also enables the simulation of hyperspectral snow reflectance measurements in the broad spectral range from ultraviolet to the near-infrared for a given snow surface in the case, if the actual measurements are performed at restricted number of wavelengths (2-4, depending on the type of snow and the measurement system).

1. Introduction

The reflective properties of clean and polluted snow are of importance for various applications including climate (Hansen and Nazarenko, 2007) and environmental pollution (Nazarenko et al., 2017) studies. The spectral snow reflectance is usually studied in the framework of the radiative transfer theory. The application of the numerical methods for the solution of the radiative transfer equation for snow layers has been performed by Mishchenko et al. (1999), Stamnes et al. (2011), and He et al. (2018) among others. The approximate solutions of the radiative transfer equation useful for snow optics and spectroscopy applications have been developed by Warren and Wiscombe (1980), Wiscombe and Warren (1980) and Kokhanovsky and Zege (2004). In this work, we propose an analytical snow albedo and reflectance model, which can be used to derive near - surface snow optical and microphysical properties using measurements at just two to four wavelengths in the visible and near–infrared depending on the measurement system and type of snow. In particular, we present the method for the determination of snow grain size, absorption Angström coefficient and spectral absorption coefficient of impurities embedded in the snow matrix assuming an external mixture of snow grains and impurities. A technique to derive the snow albedo from reflectance measurements is also presented. The absorption and extinction of light by snow grains is treated in the framework of a geometrical optical approximation. The absorption coefficient of impurities is modeled using the Angström power law. All derivations

54 are performed in the framework of the asymptotic radiative transfer theory (see, e.g.,

55 Kokhanovsky and Zege, 2004, Zege et al., 2011). It is assumed that the snow layer is vertically

56 and horizontally homogeneous and semi-infinite. Therefore, the effects of the finite layer

57 thickness are ignored.

58

59 **2. Theory**

60 **2.1 The snow reflectance**

61 The snow reflectance R (equal to unity for ideal white Lambertian reflectors, see Appendix A)

62 can be presented in the following way using approximate asymptotic radiative transfer theory

63 (Kokhanovsky and Zege, 2004):

$$R = R_0 r_s^x, \tag{1}$$

65 where $x = u(\mu_0)u(\mu)/R_0$, R_0 is the reflectance of a semi-infinite non-absorbing snow layer,

66 $u(\mu_0) = \frac{3}{7}(1 + 2\mu_0)$, μ_0 is the cosine of the solar zenith angle, μ is the cosine of the viewing

67 zenith angle, r_s is the snow spherical albedo:

$$r_s = e^{-y}, \tag{2}$$

69 where

$$y = 4\sqrt{\frac{1 - \omega_0}{3(1 - g)}}, \tag{3}$$

71 g is the asymmetry parameter, ω_0 is the single scattering albedo. Let us introduce the probability

72 of photon absorption $\beta \equiv 1 - \omega_0$. It is equal as the ratio of absorption κ_{abs} and extinction κ_{ext}

73 coefficients:

$$\beta = \frac{\kappa_{abs}}{\kappa_{ext}}, \tag{4}$$

74

75 where

$$\kappa_{abs} = \kappa_{abs}^{ice} + \kappa_{abs}^{pol}. \tag{5}$$

76

77 The first and second terms in Eq. (5) correspond to the ice grains and pollutants, respectively.

78 We assume that scattering and extinction of light by impurities is much smaller than that by ice

79 grains and, therefore (Kokhanovsky and Zege, 2004),

$$\kappa_{ext} = \frac{3c}{d}. \tag{6}$$

80

81 Here, $d = 1.5\bar{V} / \bar{S}$ is the effective diameter of ice grains, $\bar{V}$ is the average volume of grains, $\bar{S}$

82 is their average projected area averaged over all directions (equal to $\sum/4$ for convex particles in

83 random orientation, where $\sum$ is the average surface area and c is the volumetric concentration of

84 the snow grains). The value of c is equal to the volume of grains in unit volume of snow

85 ($c = N\bar{V}$, where N is the number of snow grains in unit volume of snow (cm^{-3})). It is related to

86 the dry snow density ρ_s by the following relation: $\rho_s = c\rho_i$, where ρ_i is the bulk ice density.

87   The product of the effective diameter d and the bulk ice absorption coefficient α is a small

88   number in the visible and near-infrared. Then it follows (Kokhanovsky and Zege, 2004, see their

89   Eq. (37) for the absorption path length inversely proportional to the absorption coefficient) that:

90
$$\kappa_{abs}^{ice} = B\alpha c, \tag{7}$$

91   where B is the grain shape-dependent parameter (absorption enhancement parameter),

92    $\alpha = \dfrac{4\pi\chi}{\lambda}$, where χ is the imaginary part of the ice refractive index at the wavelength λ.

93   We present the absorption coefficient of pollutants in snow as

94
$$\kappa_{abs}^{pol}(\lambda) = \kappa_0 \tilde{\lambda}^{-m}, \tag{8}$$

95   where $\kappa_0 \equiv \kappa_{abs}^{pol}(\lambda_0)$, $\tilde{\lambda} = \lambda / \lambda_0$, $\lambda_0 = 1\,\mu m$, m is the absorption Angstrom coefficient.

96   It follows from Eqs. (4)-(8):

97
$$\beta = \frac{B\alpha d}{3} + \beta^{pol}, \tag{9}$$

98   where

99
$$\beta^{pol} = \frac{\kappa_0 \tilde{\lambda}^{-m} d}{3c} \tag{10}$$

100   and therefore:

101
$$y = \frac{4}{3}\sqrt{\frac{(B\alpha + \kappa_0 \tilde{\lambda}^{-m} c^{-1})d}{1-g}}. \tag{11}$$

102   Let the parameter $z = y^2$, from which it follows that:

$$z = (\alpha + f\tilde{\lambda}^{-m})l, \tag{12}$$

104   where

$$f = \frac{\kappa_0^*}{B}, \tag{13}$$

106    $\kappa_0^* = \kappa_0 / c$ and

$$l = \xi d \tag{14}$$

108   is the effective absorption length (EAL) and

$$\xi = \frac{16B}{9(1-g)} \tag{15}$$

110   is a grain shape (but not the grain size) dependent parameter.

111   The parameter l can be determined directly from reflectance or albedo measurements, enabling

112   also the determination of the grain diameter $d = l / \xi$ assuming a particular shape of grains. It has

113   been found that the asymmetry parameter of crystalline clouds is usually in the range 0.74-0.76

114   in the visible (Garret, 2008). The asymmetry parameter g for snow has not been measured so far

115   *in situ* but we shall assume that it is close to that in crystalline clouds and adopt the value 0.75. It

116   follows from experimental studies of Libois et al. (2014) that *B=1.6* on average. Therefore, it

117   follows (see Eq. 15): $\xi \approx 11.38$.

118   Using the EAL, the equations for the snow reflectance and spherical albedo may be simplified.

119   Namely, it follows:

$$R = R_0 \exp(-x\sqrt{(\alpha + f\tilde{\lambda}^{-m})l}), \tag{16}$$

$$r_s = \exp(-\sqrt{(\alpha + f\tilde{\lambda}^{-m})l}). \tag{17}$$

122   The plane albedo can be derived as well (Kokhanovsky and Zege, 2004):

123
$$r = \exp(-u(\mu_0)\sqrt{(\alpha + f\tilde{\lambda}^{-m})l}). \tag{18}$$

124   The relationship between the albedo and the reflectance R is given in Appendix A. It follows

125   from Eq. (16) that the spectral reflectance of polluted snow is determined by four *a priori*

126   unknown parameters: l, R_0, f, m. They can be estimated from the measurements of reflectance at

127   four wavelengths. This also enables the determination of the spectral reflectance (and albedo, see

128   Eq.(18)) at the visible and near – infrared wavelengths at an arbitrary λ. It follows:

129
$$R_1 = R_0 \exp(-x\sqrt{(\alpha_1 + f\tilde{\lambda}_1^{-m})l}), \tag{19}$$

130
$$R_2 = R_0 \exp(-x\sqrt{(\alpha_2 + f\tilde{\lambda}_2^{-m})l}) \tag{20}$$

131
$$R_3 = R_0 \exp(-x\sqrt{(\alpha_3 + f\tilde{\lambda}_3^{-m})l}) \tag{21}$$

132
$$R_4 = R_0 \exp(-x\sqrt{(\alpha_4 + f\tilde{\lambda}_4^{-m})l}) \tag{22}$$

133   where the numbers 1, 2, 3, and 4 signify the wavelengths used. Equations (19)-(22) can be used

134   to compute four unknown parameters given above, and, therefore, determine reflectance and

135   albedo at any wavelength in the visible and the near-infrared using Eqs. (16)-(18). Let us assume

136   that the spectral channels are selected in a way that the effects of ice absorption can be neglected

137   in the first two channels (λ_1, λ_2) and effects of absorption by pollutants are negligible in the

138   second pair of channels (λ_3, λ_4). This situation is typical of not heavily polluted snow. Then it

139   follows instead of Eqs. (19)-(22):

140
$$R_1 = R_0 \exp(-x\sqrt{f\tilde{\lambda}_1^{-m}l}), \tag{23}$$

141
$$R_2 = R_0 \exp(-x\sqrt{f\tilde{\lambda}_2^{-m}l}), \tag{24}$$

142
$$R_3 = R_0 \exp(-x\sqrt{\alpha_3 l}), \tag{25}$$

143
$$R_4 = R_0 \exp(-x\sqrt{\alpha_4 l}). \tag{26}$$

144 Eqs. (25), (26) can be used to find the pair (l, R_0):

145
$$R_0 = R_3^{\varepsilon_1} R_4^{\varepsilon_2}, \quad l = \frac{1}{x^2 \alpha_4} \ln^2\left[\frac{R_4}{R_0}\right], \tag{27}$$

146 where $\varepsilon_1 = 1/(1-b), \varepsilon_2 = 1/(1-b^{-1}), b = \sqrt{\alpha_3/\alpha_4}$. Then it follows from Eqs. (23), (24) that:

147
$$m = \frac{\ln(p_1/p_2)}{\ln(\lambda_2/\lambda_1)}, \tag{28}$$

148
$$f = \frac{p_1 \tilde{\lambda}_1^m}{x^2 l}, \tag{29}$$

149 where $p_k = \ln^2(R_k/R_0)$. In case of the absence of pollutants, Eqs. (27) remain valid. However,

150 the parameters m and f are undefined and $R = R_0 \exp(-x\sqrt{\alpha l})$.

151 One may also derive the impurity absorption coefficient at the wavelength

152 λ_0 normalized to the concentration of ice grains c (see Eq. (13)):

153
$$\kappa_0^* = Af, \tag{30}$$

154   where f is given by Eq.(29). The normalized absorption coefficient at each wavelength can also

155   be found using Eqs. (8), (28), (30).

156   To determine the concentration of pollutants (c_p) one must either know in advance or determine

157   the impurity volumetric absorption coefficient defined as:

158
$$K(\lambda_0) = \frac{\bar{C}_{abs}(\lambda_0)}{\bar{V}},$$
(31)

159   where $\bar{C}_{abs}$ is the average absorption cross section of impurities and $\bar{V}$ is the averge volume of absorbing
160   impurities. Namely, it follows by definition:

161
$$c_p = \frac{\kappa_0}{K(\lambda_0)}$$
(32)

162

and

163
$$\mathbb{C} = \frac{\kappa_0^*}{K(\lambda_0)},$$
(33)

164   where $\mathbb{C} = c_p / c$.

165   The value of $K(\lambda_0)$ can be found, if one knows the type of pollutants and their microphysical properties.
166   In particular, it follows for the impurities much smaller than the wavelength λ_0 (van de Hulst, 1981) that :
167
$$K(\lambda_0) = F\alpha_{pol}(\lambda_0),$$
(34)

168   where

169
$$\alpha_{pol}(\lambda_0) = \frac{4\pi\chi_{pol}(\lambda_0)}{\lambda_0}$$
(35)

170   is the pollutant bulk absorption coefficient, $\chi_{pol}(\lambda_0)$ is the imaginary part of pollutant refractive

171   index and n_{pol} is the real part of the pollutant refractive index,

172

$$F = \frac{9n_{pol}}{\left(n_{pol}^2 + 1 - \chi_{pol}^2\right)^2 + 4n_{pol}^2 \chi_{pol}^2} \quad . \tag{36}$$

173   It follows that $F = 0.9$ for soot (assuming that $n=1.75$, $\chi_{pol} = 0.47$ in the visible). One can see

174   that $\mathbb{C}$ can be found if one knows the refractive index of absorbing Rayleigh particles in

175   advance.

176

In particular, it follows for soot impurities that:

177

$$\mathbb{C} = \frac{Ap_1\tilde{\lambda}_1^m}{x^2 lF\alpha_{pol}(\lambda_0)}. \tag{37}$$

178   In case of non-Rayleigh scatterers, one needs to know not only the refractive index but

179   also the particle size distribution and shape of particles, enabling the determination of the

180   impurity volumetric absorption coefficient $K(\lambda_0)$ and, therefore, the normalized concentration

181   of impurities

182

$$\mathbb{C} = \frac{Ap_1\tilde{\lambda}_1^m}{x^2 lK(\lambda_0)}. \tag{38}$$

183

184

185

2.2. The snow albedo

186   **2.2.1 Theory**

187   If the plane albedo is the measured physical quantity one needs to find only three constants:

188   $l, f, m.$

189   The respective analytical equations can be presented as:

$$r_1 = \exp(-u(\mu_0)\sqrt{(\alpha_1 + f\tilde{\lambda}^{-m})l}),$$ (39)

$$r_2 = \exp(-u(\mu_0)\sqrt{(\alpha_2 + f\tilde{\lambda}_2^{-m})l}),$$ (40)

$$r_3 = \exp(-u(\mu_0)\sqrt{(\alpha_3 + f\tilde{\lambda}_3^{-m})l}).$$ (41)

193   We shall assume that the last channel is not influenced by impurities and the first two channels

194   are not influenced by the absorption of light by grains. Then it follows that:

$$r_1 = \exp(-u(\mu_0)\sqrt{f\tilde{\lambda}_1^{-m}l}),$$ (42)

$$r_2 = \exp(-u(\mu_0)\sqrt{f\tilde{\lambda}_2^{-m}l}),$$ (43)

$$r_3 = \exp(-u(\mu_0)\sqrt{\alpha_3 l}).$$ (44)

198   The EAL can be found from Eq. (44):

$$l = \frac{\ln^2 r_3}{u^2(\mu_0)\alpha_3}.$$ (45)

200 It follows from Eqs. (42), (43) that:

$$m = \frac{\ln\left(\psi_2 / \psi_1\right)}{\ln\left(\lambda_1 / \lambda_2\right)}, \ f = \frac{\psi_1 \tilde{\lambda}_1^m}{u^2\left(\mu_0\right)l}, \tag{46}$$

202 where $\psi_k = \ln^2 r_k$.

203   In case of unpolluted snow, one derives:

$$r = \exp(-u\left(\mu_0\right)\sqrt{\alpha l}). \tag{47}$$

205 Eq. (45) can be used to find the effective absorption length and, therefore, the spectral albedo of

206 unpolluted snow at any wavelength using Eq. (47). If not plane but rather spherical albedo is

207 measured, then all equations presented in this section are valid except one should assume that

208 $u = 1$ and substitute r by r_s (Kokhanovsky and Zege, 2004).

209 **3. Experiment**

210 **3.1 The measurements of the plane albedo**

211 We have applied the technique developed above to the measured spectral plane albedo both for

212 polluted and pure snow. Therefore, in-situ spectral albedo measurements were obtained from two

213 different field sites located in the French Alps (polluted snow) and in Antarctica (clean snow).

214 *The spectral albedo of a spring alpine snowpack* was measured at the Col du Lautaret field site

215 (45°2' N, 6°2' E, 2100 m a.s.l.) in the French Alps. The measurements were performed using a

216 non-automated version of the spectrometer system described above. The hand-held instrument

217 has a single light collector, located at the end of 3 m boom placed 1.5 m above the surface. The

218 boom is rotated by the operator to successively acquire the downward and upward solar

219   radiation. The spectral albedo data (each spectral albedo measurement at a given point is an

220   average of five measurements) at several locations close to the location Col du Lautaret field site

221   was obtained on 12th April, 2017 across a 100 m transect, in attempt to account for spatial

222   variability. The measurements were acquired in clear sky conditions, with a solar zenith angle

223   varying between 47.9º and 52.2º.

224   The results of comparison of measurements and the theory presented above are illustrated in

225   Fig.1 at the Col du Lautaret field site. The parameters l, f, m have been found from Eqs. (42)-

226   (44) and the measurements at the wavelengths $\lambda_1 = 400nm, \lambda_2 = 560nm, \lambda_3 = 1020nm$. At other

227   measurement sites across a transect the results of the inter-comparison are excellent and similar

228   to that presented in   Fig.1. Therefore, the theory can be used to derive snow optical and

229   microphysical properties even for polluted snowpack. The derived spectral probability of photon

230   absorption for the case shown in Fig. 1 is presented in Fig.2. The derived absorption coefficient

231   (assuming c=1/3), the grain diameter d and the absorption Angström parameter m for five sites

232   across the transect are listed in Table 1 (lines 1-5). It follows that the value of m is in the range

233   2.4 - 4.1 consistent with the identified presence of dust particles in snow (Doherty et al., 2010).

234   The pure black carbon impurities have the values of m close to one. The grain diameter is in the

235   range 1.7-2.2 mm consistent with low values of snow albedo at 1020nm (see Fig.1). Wiscombe

236   and Warren (1981) have calculated the dependence of the clean snow spectral albedo at the solar

237   zenith angle 60 degrees and several grain radii and presented it in their Fig.8. It follows from

238   their calculations that the albedo decreases from 0.8 to 0.4 while the diameter of grains changes

239   from 0.1 to 2mm. It follows from our Fig.1 that the measured plane albedo is close to 0.45

240   signifying the dominance of large grains in the snowpack as reported in Table 1.

241 *The spectral albedo of pure snow* (very low amount of impurities) was measured at Dome C

242 (75°5' S, 123°17' E), in Antarctica using an automated spectral radiometer (Libois et al., 2015;

243 Picard et al., 2016; Dumont et al., 2017). The instrument is composed of two individual heads

244 located approximately 1.5 m above the surface. Each head contains two cosine receptors facing

245 upward and downward, which receive the incident solar radiation and the reflected radiation. The

246 collectors are connected to a MAYA2000 PRO Ocean Optics spectrometer with fibre optics

247 through an optical switch. Radiation is measured over 350-1100 nm spectral range with an

248 effective spectral resolution of 3 nm. Albedo was calculated as the ratio of the upward and

249 downward spectral irradiance. The full description of the instrument and the processing steps to

250 calculate the spectral albedo are given by Picard et al. (2016). The spectral albedo measurements

251 used here were made on the 10th January 2017, with a solar zenith angle of 63.2º, during clear

252 sky conditions assessed by ground observations.

253 The results of the application of the proposed technique to the pure snow (no pollution) albedo

254 measured in Antarctica are illustrated in Fig.3. Application of our technique results in excellent

255 agreement with measured albedo over pure snow (now pollution) in Antarctica. Because the

256 snow at Dome C is clean/pristine, the value of *f* is negligible, resulting in snow albedo depending

257 only on the effective absorption length/grain size, which has been derived at a single wavelength

258 (1020nm). The derived grain diameter for the case presented in Fig.3 is equal to 0.5mm. The

259 retrieval error estimation is presented in Appendix B.

260

261

262

3.2 The measurements of the spectral reflectance

The application of the developed theory to the measurements of the spectral reflectance is presented in Fig.4 for two locations with different dust loads (39.6ppm and 107.4ppm). The spectral reflectance of snow was measured in the European Alps (Artavaggio plains, 1650m a.s.l., 45°55'56.70"N; 9°31'33.28" E) at the solar zenith angle equal to 52 degrees. The measurements were made on March 14th 2014, after a major transport and deposition of mineral dust from the Saharan desert. The event was very intense, and it was reported in the recent scientific literature regarding snow optical properties, (Di Mauro et al., 2015; Dumont et al., 2017), atmospheric chemistry and physics (Belosi et al., 2017), and also microbiology (Weil et al., 2017). The dust transport event deposited fine mineral dust particles from the atmosphere via wet deposition, according to the BSC-DREAM-8b model (Basart et al., 2012). Spectral measurements of snow were made using a field spectrometer (Field Spec Pro, Analytical Spectral Devices, ASD). This instrument features a spectral range of 350-2500 nm, a full width at half maximum of 5–10 nm, and a spectral resolution of 1 nm. Data presented here were collected under clear sky conditions at noon. Incident radiation was estimated using a Lambertian Spectralon panel. Reflected radiance was divided by incident radiance, and the hemispherical conical reflectance factor was calculated for two plots containing 39.6 and 107.4 ppm of dust. Dust concentration was measured with a Coulter Counter by integrating particles with a diameter smaller than 18 μm. Spectral measurements were performed at nadir using a bare optical fiber (field of view of 25°) at 80 cm from the snow sample. Both the optical fiber and the spectralon panel were equipped with an optical level. Further details on this dataset can be found in Di Mauro et al. (2015).

285   One can see that the theory works well not only for the albedo measurements (see the

286   previous section) but also for the reflectance measurements for polluted snow layers. In

287   particular, our results are closer to the measurements as compared to the theoretical model

288   described by Flanner et al. (2007) (see Fig.4b in Di Mauro et al., 2015). The derived parameters

289   are given in Table 1 (lines 6-7). The value of m is *4.1* for the case with the 39.6ppm dust

290   concentration and it is *6.4* for the case with 107.4 dust concentration. Because the difference is

291   quite large for the close locations we conclude that snow also contained other pollutants (say,

292   soot) and the determined value of *m* represents the combined effect with larger values of *m* for

293   larger concentrations of dust, which is consistent with other observations of this parameter in

294   snow (Doherty et al., 2010). The retrieved absorption coefficient of snow pollutants (at the

295   wavelength $\lambda^* = 560 nm$) is $0.1191 \, m^{-1}$ for the dust concentration 39.6ppm and it is $0.3123 \, m^{-1}$

296   for the dust concentration of 107.4 ppm. Assuming that the dust chemical composition and also

297   the dust particle size distribution are the same at both locations we can assume that the ratio of

298   absorption coefficients at two locations should be equal to the ratio of dust concentrations. The

299   difference between the two ratios is <3%, which is within the measurement uncertainty (10% for

300   dust load measurements), and suggesting that the retrieved absorption coefficients at the two

301   sites are consistent with each other.

302   The mass absorption coefficient (MAC) can be estimated using:

303
$$K_m = \frac{\kappa_{abs}^{pol}\left(\lambda^*\right)}{\mathbb{C}\rho c},$$
(48)

304   where ρ is the density of the substance of impurities. Assuming that:

305     $\rho = 2.62 g / cm^3$ (as for quartz), $c = 1/3$, $\mathbb{C} = 107.4 \, ppm$ and $\kappa_{abs}^{pol}\left(\lambda^*\right) = 0.3123 m^{-1}$,
(49)

306   one can derive that:

$$K_m = 0.0033 m^2 / g, \qquad (50)$$

308   which is consistent with the values of MAC given by Utry et al.(2015) (e.g.,

309    $0.0023 m^2 / g$ for quartz and $0.0051 m^2 / g$ for illite (see their Table 1)).

4. Conclusions

311   In this work, we have presented a sequence of analytical equations, which can be used to

312   determine the snow grain size, the absorption coefficient of impurities, and the absorption

313   Angström coefficient of surface snow impurities from the snow reflectance measured at four

314   wavelengths: two in the visible and two in the near infrared as suggested by Warren (2013). In

315   the case of albedo measurements just three wavelengths can be used to find main snow

316   properties. For unpolluted snow, it is enough to perform the measurements at two wavelengths

317   (for reflectance measurements) or just at a single wavelength (for albedo measurements) in the

318   near-infrared to determine the snow grain size.

319   In principle, the refractive index of dust and dust size distribution can be also determined using

320   derived spectral absorption coefficient of dust and assuming the shape of dust particles.

321   However, we did not make an attempt for such retrievals in this work. The method for the

322   retrieval of the complex refractive index and single scattering optical properties of dust deposited

323   in mountain snow based on exact radiative transfer calculations has been proposed by McKenzie

324   Siles et al. (2016) in the assumption that local optical properties of dust grains can be simulated

325   assuming the spherical shape of particles. Their method is based on the extraction of dust grains

326   from snowpack. Our technique does not require such a complicated procedure.

327   We have demonstrated how snow albedo can be derived from spectral reflectance measurements

328   avoiding complicated integration with respect to the observation geometry (azimuth, viewing

329   angle). The last point is useful for the determination of the snow *albedo* from spectral *reflectance*

330   measurements (say, from aircraft or satellite) at a fixed observation geometry. Although the

331   comprehensive validation of the retrievals has not been attempted, we have found that the ratio

332   of derived absorption coefficients of pollutants at two concentrations is close to the ratio of

333   pollutant concentrations derived independently, which indeed should be the case taking the

334   proximity of two measurement sites with different dust loads. The general validity of the

335   approach is proven using field measurements (Alps, Antarctica) of both spectral reflectance and

336   plane albedo.

337   The determination of the EAL l (unlike the effective grain diameter d) both from reflectance

338   and albedo measurements is practically insensitive to the *a priori* unknown shape of ice crystals.

339   Therefore, this length may be useful for the characterization of snowpack microstructure (in

340   addition to the grain size d). The results presented in this work are useful for the interpretation of

341   snow properties using both reflectance spectroscopy (Hapke, 2005) and imaging spectrometry

342   (Dozier et al., 2009). It is assumed that the semi - infinite snow layer is vertically and

343   horizontally homogeneous. The effects of the snow layer finite thickness, close packing effects,

344   snow vertical inhomogeneity, possible internal mixture of pollutants in snow grains, and

345   underlying surface albedo (ice, soil, grass) are ignored.

346

347

348

350 **Appendix A. Nomenclature**

Physical parameter	Notation	Units	Definition	Comments
Snow absorption coefficient	κ_{abs}	m^{-1}	$N\bar{C}_{abs}$	N -number of snow grains in unit volume(m^{-3}) $\bar{C}_{abs}$ -average absorption cross section of grains (m^2)
Snow extinction coefficient	κ_{ext}	m^{-1}	$N\bar{C}_{ext}$	N -number of snow grains in unit volume(m^{-3}) $\bar{C}_{ext}$ -average extinction cross section of grains (m^2)
Probability of photon absorption	β	-	$\kappa_{abs}/\kappa_{ext}$	$\beta \ll 1$ in the approximation studied
Snow single scattering albedo	ω_0	-	$1-\beta$	close to 1 in the approximation studied
Snow asymmetry parameter	g	-	$g = \frac{1}{2}\int_0^\pi p(\theta)\sin\theta\cos\theta d\theta$	$\frac{1}{2}\int_0^\pi p(\theta)\sin\theta d\theta = 1$ θ is the scattering angle(equal to π in the exact backward scattering direction) $p(\theta)$ is the conditional probability of photon scattering in a given direction specified by the angle θ (phase function)
Bulk ice absorption coefficient	α	m^{-1}	$\frac{4\pi\chi(\lambda)}{\lambda}$	$\chi(\lambda)$ - imaginary part of bulk ice refractive index λ - wavelength
Volumetric absorption coefficient of pollutants	K	m^{-1}	$\bar{C}_{abs}^{pol}/\bar{V}_p$	$\bar{C}_{abs}^{pol}$ -average absorption cross section of impurities in snow (m^2), $\bar{V}_p$ is their average volume(m^3), K is _proportional_ to the bulk absorption coefficient of impurities in case they are much larger as compared to

				the wavelength (and weakly absorbing) or much smaller as compared to the wavelength (so called Rayleigh scatterers). The coefficient of proportionality (absorption enhancement factor) depends on the shape of particles and real part of their complex refractive index.
Effective absorption length	l	m^{-1}	$\dfrac{\ln^2 r_s}{\alpha}$ (for clean dry snow)	$r_s = \exp(-\sqrt{\alpha l})$ r_s -spherical albedo α -bulk ice absorption coefficient This definition holds for clean dry snow only The general definition for dry snow is given by Eq. (17)
Reflectance	$R(\mu_0,\mu,\varphi)$	-	$I^{\uparrow}(\mu_0,\mu,\varphi)/I^{\uparrow}_{Lamb}(\mu_0)$	Ratio of intensity of light reflected from a given snowpack to that of an ideal Lambertian surface with albedo 1.0 (μ_0,μ,φ) -cosine of the solar zenith angle, cosine of viewing zenith angle, and relative azimuth, respectively
Plane albedo	$r(\mu_0)$	-	$2\int_0^1 \bar{R}(\mu_0,\mu,\varphi)\mu d\mu$	$\bar{R}=\dfrac{1}{2\pi}\int_0^{\pi} R(\mu_0,\mu,\varphi)\varphi d\varphi$ - reflectance averaged with respect to the azimuth, black sky albedo
Spherical albedo	r_s	-	$2\int_0^1 r(\mu_0)\mu_0 d\mu_0$	white sky albedo
Volumetric concentration of grains	c	-	$N\bar{V}$	N – number concentration of grains, $\bar{V}$ -average volume of grains, c - fraction of unit volume occupied by ice grains (usually around 0.3)
Mass concentration of	ρ_s	gm^{-3}	$N\bar{m}$	N – number concentration of grains,

grains (snow density)				$\bar{m} = \rho_i \bar{V}$ -average mass of grains, ρ_i - bulk ice density, $\rho_s = \rho_i c$ (for dry snow)
Bulk ice density	ρ_i	gm^{-3}	-	$\rho_i = 916.7 kg/m^3$ at $0^\circ C$
Bulk pollutant density	ρ_p	gm^{-3}	-	
Volumetric concentration of impurities	c_p	-	$N_p \bar{V}_p$	N_p – number concentration of pollution particles, $\bar{V}_p$ -average volume of pollution particles, c - fraction of unit volume occupied by impurities
Normalized volumetric concentration of impurities	$\mathbb{C}$	-	c_p / c	$\mathbb{C} = \dfrac{\rho_i}{\rho_s} c_p$ ρ_i - bulk ice density, ρ_s - snow density, c_p - volumetric concentration of impurities
Effective diameter of grains	d	m	$\dfrac{3\bar{V}}{2\bar{S}}$	equal to the diameter for the collection of spherical grains of the same size, $\bar{V}$ -average volume of grains, $\bar{S}$ -average cross section of grains (perpendicular to incident light beam),

351

352

353

354

355

356

357

358   **Appendix B. The retrieval error estimation**

359   **1. The effective absorption length and diameter of grains**

360   Let us consider the error budget for the retrieved snow parameters. To simplify, we assume that

361   the snow parameters are derived using albedo measurements.

362   The value of l is determined from measurements just at a single wavelength in the framework of

363   the theory given above. It follows from Eq. (45):

364
$$\frac{\Delta l}{l} = K \frac{\Delta r_3}{r_3},$$
(B.1)

365   where

366
$$K = \frac{2}{\ln r_3}.$$
(B.2)

367   Therefore, the relative effective absorption length retrieval error is directly proportional to the

368   relative measurement error in the measured albedo. Larger values of l correspond to the smaller

369   albedo. So one would conclude that that the error of retrieval of larger values of EAL are

370   generally smaller (see Eq.(B.2)). For the cases presented in Figs. 1 and 2, the wavelength

371   1020nm has been used in the retrieval process and one finds that K is equal to -2.5 and -5.8,

372   respectively. Assuming the measurement error of 3%, one derives that EAL is determined with

373   accuracies of -7.5 and -17.4 %, respectively, with better accuracy for the observations in Alps,

374   because the albedo is lower there. Also we see that the overestimation of the albedo in the

375   experiment leads to the underestimation of the EAL, and other way around in the case

376   measurements which underestimate the snow albedo because K is negative. Because K generally

377 decreases with the wavelength one must use the largest wavelengths to have better accuracy (say,

378 1020nm instead of 865nm). The wavelength should not be above 1200nm or so (depending on

379 the snow grain size) because the underlying theory valid for weakly absorbing media only. So

380 strong ice absorption bands must be avoided. The value of the snow grain size is proportional to

381 the value of l. Therefore, our conclusions are also valid for the derived snow grain size assuming

382 that one knows the parameter ξ (see Eq.15) exactly. However, this parameter is known with

383 some error.

384 The uncertainty in the parameter $\xi = 16B/3(1-g)$ is difficult to access because we rely on a priori

385 value for the snow asymmetry parameter and the absorption enhancement parameter B. We use

386 the following values: $B=1.6, g=0.75$. The reported values of g for   crystalline clouds do not go

387 above 0.8. Therefore, the modulus of the absolute error in the parameter $1-g$ is smaller than 0.05

388 (and the relative error is below 20%). The value of B is usually in the range: 1.4-1.8 and,

389 therefore, the absolute error in the parameter B is equal approximately to ± 0.2 and, therefore,

390 the relative error is $\pm 12.5\%$. It follows that the absolute value of the maximal relative error in

391 the parameter ξ is close to 24%. The error could be smaller in case the assumptions used in the

392 derivations are closer to the actual snow conditions. We find that the maximal relative error in

393 the derived grain diameter for the cases shown in Fig. 1, 2 is 25-30% depending on the snow

394 type, which is substantially larger as compared to the error in the estimation of EAL.

395

396

397

398

2. The spectral absorption coefficient of pollutants

Let us consider the error budget for the retrieved spectral absorption coefficient of
pollutants. The absolute error of the retrieved parameter Δx is defined as

$$\Delta x = \sqrt{\sum_{j=1}^{J} \left[\frac{\partial x}{\partial y_j}\right]^2 \Delta y_j^2} \ . \tag{B.3}$$

This error depends on j measurement errors of reflectance/albedo at j-channel Δy_j , where J is
the number of channels used to retrieve the corresponding parameter assuming that there are no
forward model errors. It a difficult task to estimate the forward model error theoretically. It
depends on the specific type of snowpack.

It follows from Eqs. (46), (B.3) :

$$\frac{\Delta f}{f} = \sqrt{\Upsilon_1^2 \left[\frac{dr_1}{r_1}\right]^2 + \Upsilon_3^2 \left[\frac{dr_3}{r_3}\right]^2}, \quad \frac{\Delta m}{m} = \sqrt{\Pi_1^2 \left[\frac{dr_1}{r_1}\right]^2 + \Pi_2^2 \left[\frac{dr_2}{r_2}\right]^2}, \tag{B.4}$$

where

$$\Upsilon_n = \frac{2}{\ln r_n}, \ \Pi_n = \frac{2}{\ln r_n \ln\left(\psi_2 / \psi_1\right)}. \tag{B.5}$$

We conclude that the errors of the pair (f, m) determination increase, if the selected wavelengths
at two channles in the visible   are too close and if the logarithm of albedo at selected channels is
close to unity (say, weak concentration of pollutants for the channels in the visible). The albedo

414

decreases for the cases with illumination closer to nadir. Therefore, to reduce errors one needs to

415

use measurements with larger deviations of Sun from the horizon direction.

416

The absorption coefficient of pollutants is given by the following equation (see Eqs. (8),

417

(13),(30)):

418

$$\kappa_{abs}^{pol} = Bcf\,\tilde{\lambda}^{-m}.$$

(B.6)

419

Therefore, one derives

420

$$\frac{\Delta\kappa_{abs}^{pol}}{\kappa_{abs}^{pol}} = \sqrt{\left[\frac{\Delta B}{B}\right]^2 + \left[\frac{\Delta f}{f}\right]^2 + \left[\frac{dc}{c}\right]^2 + \ln^2\left(\tilde{\lambda}\right)\left[\frac{\Delta m}{m}\right]^2}.$$

(B.7)

421

One concludes that the errors in the estimated snow volumetric concentration c (snow density,

422

see Appendix A), the absorption enhancement coefficient B, and also pair (f,m) must be

423

combined to estimate the total error in the retrieved spectral absorption coefficient of impurities

424

in snow. The errors are lower, if one is interested in the spectral absorption coefficient of

425

impurities normalized to its value at a specific wavelength defined as

426

$$\tilde{\kappa}_{abs}^{pol} \equiv \frac{\tilde{\kappa}_{abs}^{pol}\left(\lambda\right)}{\tilde{\kappa}_{abs}^{pol}\left(\lambda_*\right)},$$

(B.8)

427   where λ_* is the selected wavelength (say, 550nm).

428

One derives for this coefficient:

429
$$\tilde{\kappa}_{abs}^{pol}(\lambda) \equiv \left(\frac{\lambda}{\lambda_*}\right)^{-m}$$

(B.9)

430

and, therefore, only the accuracy of the determination of absorption Angström exponent

431

influences the result:

432
$$\frac{\Delta\kappa_{abs}^{pol}}{\kappa_{abs}^{pol}} = \ln(\lambda/\lambda_*)^{-m}\frac{\Delta m}{m}.$$

(B.10)

433

An important point is the determination of the concentration of pollutants in snow from optical

434

remote sensing data. In principle the concentration of pollutants can be found, if the absorption

435

coefficient of pollutants at a given wavelength is known. For instance,   it follows by definition

436

(see Eq. (31) for the definition of the volumetric absorption coefficient of impurities K):

437
$$c_p = \frac{\kappa_{abs}^{pol}(\lambda)}{K(\lambda)}.$$

438

Therefore, uncertainty in the derived or assumed value of K (or mass extinction coefficient

439    $K_m = K/\rho_p$, where ρ_p is the density of the substance of a pollutant) influences the retrieval error

440   in addition to uncertainty of the derived absorption coefficient of pollutants $\kappa_{abs}^{pol}(\lambda)$. One can see

441   that the determination of the concentration of pollutants from optical remote sensing of

442   snowpack is a very challenging task.

443

In particular, one finds that the positive bias in the measured albedo in the visible will lead to

444

the underestimation of the concentration of pollutants (assuming that the grain size is exactly

445

known). It should be pointed out that in most cases the concentration of pollutants is so small

446

that it can not be assessed using optical instruments (change in reflectance is inside experimental

447

measurement error). This issue has been discussed by Zege et al. (2011) and Warren (2013).

448

Similar conclusions hold also if the reflectance (and not albedo) is the measured quantity.

449

450 **5. Acknowledgments**

451 This work was mainly supported by the European Space Agency in the framework of ESRIN

452 contract No. 4000118926/16/I-NB ''Scientific Exploitation of Operational Missions (SEOM)

453 Sentinel-3 Snow (Sentinel-3 for Science, Land Study 1: Snow)''. CNRM/CEN and IGE are part of

454 labex OSUG@2020. Measurements in the French Alps were funded by the ANRJCJ grant EBONI

455 16-CE01-0006 and at Dome C by ANR JCJC MONISNOW 1-JS56-005-01.

456

References

457   **References**

458   S. Basart, S., C. Pérez, S. Nickovic, E. Cuevas, and J. M. Baldasano, ''Development and

459   evaluation of the BSC-DREAM8b dust regional model over Northern Africa, the Mediterranean

460   and the Middle East'', *Tellus B*, vol. 64, 2012, doi:10.3402/tellusb.v64i0.18539, 2012.

461   F. Belosi, M. Rinaldi, S. Decesari, L. Tarozzi, A. Nicosia, A., and G. Santachiara, ''Ground

462   level ice nuclei particle measurements including Saharan dust events at a Po Valley rural site

463   (San Pietro Capofiume, Italy)'',   *Atmospheric Research*, vol. 186, pp. 116–126,

464   https://doi.org/10.1016/J.ATMOSRES.2016.11.012, 2017.

465   B. Di Mauro, F. Fava, L. Ferrero, R.Garzonio, G.Baccolo, B.Delmonte, and R. Colombo,

466   ''Mineral dust impact on snow radiative properties in the European Alps combining ground,

467   UAV, and satellite observations'', *J. Geophys. Res. Atmos.*, vol.120, pp. 6080–6097,

468   doi:10.1002/2015JD023287, 2015.

469   S. J. Doherty, S. G. Warren, T. C. Grenfell, A. D. Clarke, and R.E. Brandt, ''Light-absorbing

470   impurities in Arctic snow'', *Atmos. Chem. Phys.*, vol.10, 11647-11680, 2010.

471   J. Dozier, R. O. Green, A. W. Nolin, and T. H. Painter, ''Interpretation of snow properties from

472   imaging spectrometry'', *Remote Sens. Env.,* vol. 113, pp. S25-S37, 2009.

473   M. Dumont, L. Arnaud, G. Picard, Q. Libois, Y. Lejeune, P. Nabat, and S. Morin, S. ''In situ

474   continuous visible and near-infrared spectroscopy of an alpine snowpack''. *The Cryosphere*,

475   vol. 11, N3, pp. 1091–1110, https://doi.org/10.5194/tc-11-1091-2017, 2017.

M. G. Flanner, C. S. Zender, J. T. Randerson, and P. J. Rash, ''Present – day climate forcing and response from black carbon in snow'', *J. Geophys. Res Atmos.*, vol.112, D11202, doi: 10.1029/2006JD008003, 2007.

T. J. Garrett, ''Observational quantification of the optical properties of cirrus cloud'', Light Scattering Reviews (ed. by A. Kokhanovsky), 3, 1-26, Praxis-Springer, 2008.

J. Hansen, and L. Nazarenko, 2004: ''Soot climate forcing via snow and ice albedos'', *Proc. Natl. Acad. Sci.*, 101, 423-428, doi:10.1073/pnas.2237157100, 2004.

B. Hapke, *Theory of reflectance and emittance spectroscopy*, Cambridge: Cambridge University Press, 2005.

C. He, K.-N. Liou, Y. Takano, P. Yang, L. Qi, and F. Chen, ''Impact of grain shape and multiple black carbon internal mixing on snow albedo: parameterization and radiative effect analysis'', *J. Geophys. Res.*, 123, 1253-1268, 2018.

A. A. Kokhanovsky, E.P. Zege, ''Scattering optics of snow'', *Appl. Optics*, vol. 43, N7, pp.1589-1602, 2004.

Q. Libois, G. Picard, M. Dumont, L. Arnaud, C. Sergent, E. Pougatch, M. Sudul, and D. Vial, " Experimental determination of the absorption enhancement parameter of snow", *J. Glaciology,* 60, N 222, 2014.

Q. Libois, G. Picard, L. Arnaud, M. Dumont, M. Lafaysse, S. Morin, and E. Lefebvre,"Summertime Evolution of Snow Specific Surface Area close to the Surface on the Antarctic Plateau," *The Cryosphere*, 9, N6, 2383-2398, 2015.

S. McKenzie Skiles, T. Painter, G. S. Okin, "A method to retrieve the spectral compex refractive

497 index and single scattering optical properties of dust deposited in mountain snow'', J.
498   Glaciology, 63, N237, 133-147.

499 M. I. Mishchenko, J.M. Dlugach, E.G. Yanovitskij, and N.T. Zakharova, ''Bidirectional
500 reflectance of flat, optically thick particulate layers: An efficient radiative transfer solution and
501 applications to snow and soil surfaces'', *J. Quant. Spectrosc. Radiat. Transfer*, vol. 63, pp. 409-
502 432, doi:10.1016/S0022-4073(99)00028-X, 1999.

503 Y. Nazarenko, S. Fournier, U. Kurien, R. B. Rangel-Alvarado, O. Nepotchatykh, P. Seers, P. A.
504 Ariya, ''Role of snow in the fate of gaseous and particulate exhaust pollutants from gasoline-
505 powered vehicles''. *Environmental Pollution*, 223, 665 DOI: 10.1016/j.envpol.2017.01.082,
506 2017

507 G. Picard, Q. Libois, L. Arnaud, G. Verin, and M. Dumont, "Development and calibration of an
508   automatic spectral albedometer to estimate near-surface snow SSA time series." *The*
509   *Cryosphere*,, 10, N3, 1297-1316, 2016.

510 K. Stamnes, B. Hamre, J. J. Stamnes, G. Ryzikov, C. Biryulina, R. Mahoney, B. Haus, and A.
511 Sei, ''Modeling of radiation transport in coupled atmosphere-snow-ice-ocean systems'', *J.*
512 *Quant. Spectrosc. Radiat. Transfer*, 112, 714-726, 2011.

513 N. Utry, T. Ajtai, M. Pinter, E. Tombacz,E. Illes, Z. Bozoki, and G. Szabo, ''Mass-specific
514 optical absorption coefficients and imaginary part of the complex refractive indices of mineral
515 dust components measured by a multi-wavelength photoacoustic spectrometer'', *Atmos. Meas.*
516 *Techniques*, 8, 401-410, 2015.

517 H. C. Van de Hulst, *Light scattering by small particles*, N.Y: Dover, 1981.

518   S. G. Warren, W. J. Wiscombe, ''A model for spectral albedo of snow: II. Snow containig

519   atmospheric aerosols'', *J. Atmos. Sci*., vol. 37, pp. 2734-2745, 1980.

520   S. G. Warren, ''Can black carbon in snow be detected by remote sensing'', *J. Geophys. Res.,*

521   *Atmospheres,* 118, 779-786, 2013.

522   T. Weil, C. De Filippo, D. Albanese, C. Donati, M. Pindo, L. Pavarini, and F. Miglietta, ''Legal

523   immigrants: invasion of alien microbial communities during winter occurring desert dust

524   storms'', *Microbiome*, vol. 5, No 1, https://doi.org/10.1186/s40168-017-0249-7, 2017.

525   W. J. Wiscombe, and S. G. Warren, ''A model for spectral albedo of snow: I. Pure snow'', *J.*

526   *Atmos. Sci.*, vol. 37, pp. 2712-2733.

527   E. P. Zege, I. L. Katsev, A. V. Malinka, A. S. Prikhach, G. Heygster, and H. Wiebe, ''Algorithm

528   for retrieval of the effective snow grain size and pollutants amount from satellite

529   measurements'', *Rem. Sens. Env.,* 115, 2674-2685.

530

531

532   Tables

533

534   Table 1. The derived snow parameters for the five samples. The value of c is assumed to be equal

535   1/3, which leads to the extinction length ($l_{ext} = 1/\kappa_{ext}$) to be equal to the effective grain diameter

536   d. The absorption coefficient is given at the wavelengths $\lambda_0 = 1000$nm and $\lambda^* = 560nm$.

537	N	$\kappa_{abs}^{pol}(\lambda_0), m^{-1}$	$\kappa_{abs}^{pol}(\lambda^*), m^{-1}$	m	d, mm	Site
538	1	0.0182	0.1954	4.1	2.1	Col du Lautaret (site 1)
539	2	0.0342	0.2668	3.5	2.2	Col du Lautaret (site2)
540	3	0.1073	0.7194	3.3	1.7	Col du Lautaret (site 3)
541	4	0.0769	0.5324	3.3	1.9	Col du Lautaret (site 4)
542	5	0.0943	0.3848	2.4	2.2	Col du Lautaret (site 5)
543	6	0.0111	0.1191	4.1	2.5	Artavaggio plains (site 1)
544	7	0.0077	0.3123	6.4	1.5	Artavaggio plains (site 2)

545

546

547

548

549   Figures
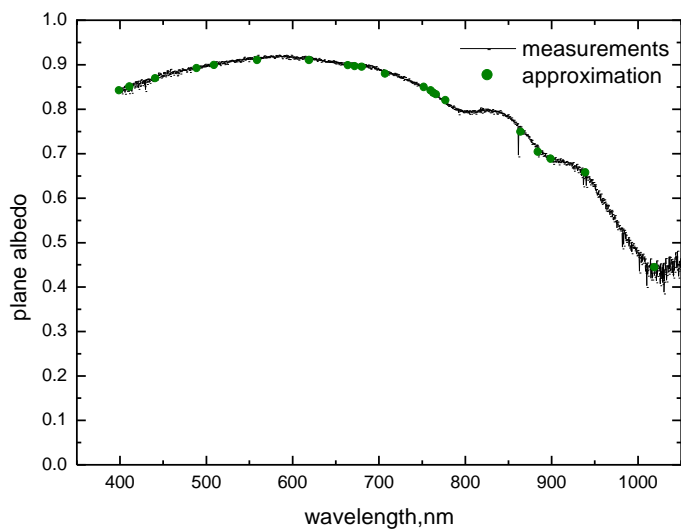
550

551   Fig.1. The intercomparison of theory (symbols) with experimental measurements of plane albedo

552   (line, no noise removed) performed in French Alps (45°2' N, 6°2' E, 2100 m a.s.l.) obtained on

553   12/04/2017. The plane albedo is an average of 5 measurements performed between 08h55 and

554   09h30 UTC for a polluted (by dust) snowpack. The solar zenith angle for the measurements was

555   between 47° and 49°. The noise of measurements has not been removed and clearly seen in the

556   near infrared portion of the spectrum.

557
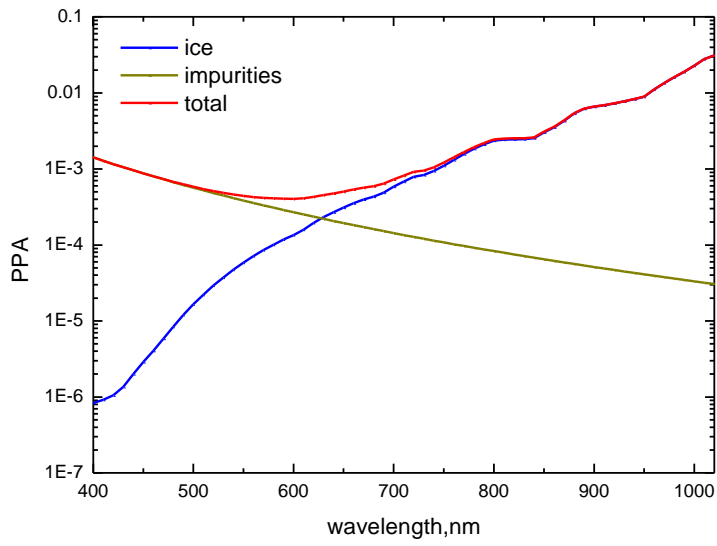
558
559

560   Fig.2. The derived spectral probability of photon absorption for the case presented in Fig.1.

561

562

563
564
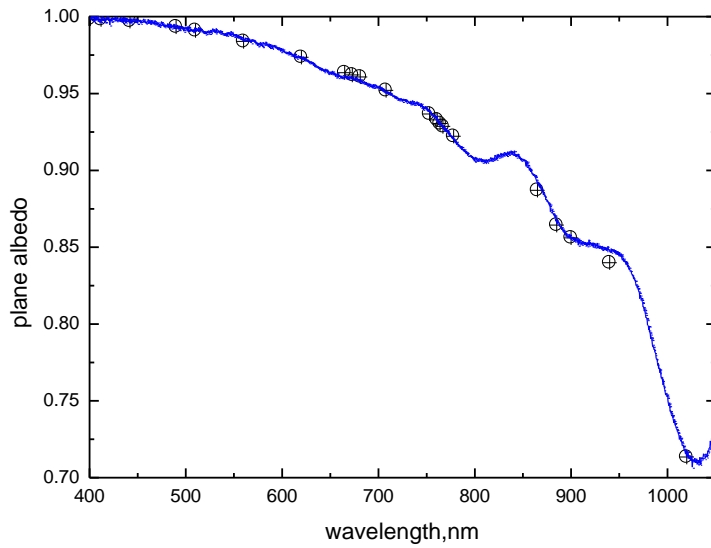
Fig.3 The inter-comparison of theory (symbols) with experimental measurements of plane albedo

(line) performed in Antarctica (Dome C, 75°5' S, 123°17' E) for pure snow. The measured plane

albedo was obtained on 10/01/2017 at 23h24 UTC, for a solar zenith angle of 63 degrees. The

parameters *l, f, m* have been derived from the measurements at 400, 560, and 1020nm.

569

570

571
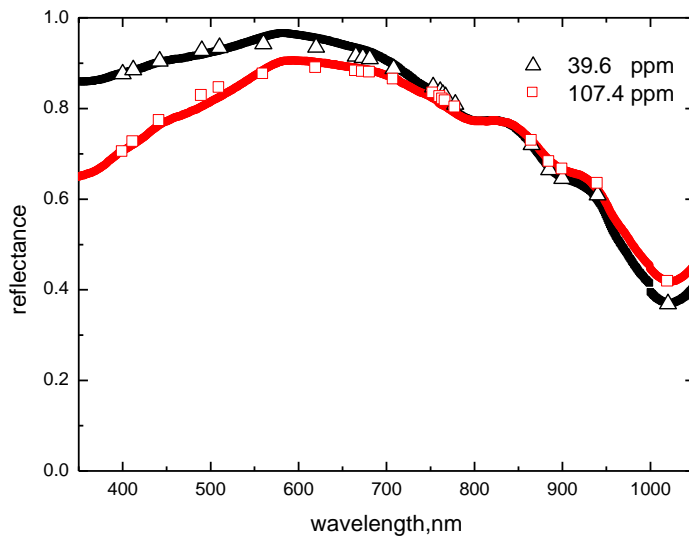
Fig.4 The inter-comparison of theory (symbols) with experimental measurements (line) in European Alps (45°55'56.70"N; 9°31'33.28" E) for the polluted snowpack. The parameters R_0, l, f, m have been derived from the measurements at 400, 560, 865 and 1020nm. Reflectance measurements were collected on snow containing different concentration of dust: 39.6 ppm (black line) and 107.4 ppm (red line). The dust has been collected from the upper snow layer ($\approx$5cm). Snow was clean at larger depths. A complete description of this dataset is presented in Di Mauro et al. (2015).

579